Nanoemulsion-induced enzymatic crosslinking of tyramine-functionalized polymer droplets

Kamperman, T.; Henke, S.; Zoetebier, B.; Ruiterkamp, N.; Wang, R.; Pouran, Behdad; Weinans, Harrie; Karperien, M.; Leijten, J

DOI
10.1039/C7TB00686A

Publication date
2017

Document Version
Accepted author manuscript

Published in
Journal of Materials Chemistry B

Accepted Author Manuscript of http://dx.doi.org/10.1039/C7TB00686A (RSC)

Nanoemulsion-induced Enzymatic Crosslinking of Tyramine-functionalized Polymer Droplets

Tom Kamperman†, Sieger Henke†, Bram Zoetebier, Niels Ruiterkamp, Rong Wang, Behdad Pouran, Harrie Weinans, Marcel Karperien, and Jeroen Leijten**

T. Kamperman M.Sc., Dr. S. Henke, Dr. B. Zoetebier, N. Ruiterkamp B.Sc., Dr. R. Wang, Prof. Dr. M. Karperien, Dr. J. Leijten

Department of Developmental BioEngineering, MIRA Institute for Biomedical Technology and Technical Medicine, University of Twente, Drienerlolaan 5, 7522NB Enschede, The Netherlands.

Email: h.b.j.karperien@utwente.nl, j.c.h.leijten@utwente.nl

Dr. R. Wang

Department of Complex Tissue Regeneration, MERLN Institute, Maastricht University, Universiteitssingel 40, 6229 ER Maastricht, The Netherlands

B. Pouran M.Sc., Prof. Dr. H. Weinans

Department of Orthopedics, UMC Utrecht, Heidelberglaan 100, 3584CX Utrecht, The Netherlands.

Department of Biomechanical Engineering, Faculty of Mechanical, Maritime, and Materials Engineering, Delft University of Technology (TU Delft), Mekelweg 2, 2628CD Delft, The Netherlands

Prof. Dr. H. Weinans

Department of Rheumatology, UMC Utrecht, Heidelberglaan100, 3584CX Utrecht, The Netherlands

† TK and SH contributed equally to this work

* JL and MK are shared senior author

Keywords: emulsions; hydrogels; microfluidics; cell encapsulation; 3D culture

Abstract

In situ gelation of water-in-oil polymer emulsions is a key method to produce hydrogel particles. Although this approach is in principle ideal for encapsulating bioactive components such as cells, the oil phase can interfere with straightforward presentation of crosslinker molecules. Several approaches have been developed to induce in-emulsion gelation by exploiting the triggered generation or release of crosslinker molecules. However, these methods typically rely on photo- or acid-based reactions that are detrimental to cell survival and functioning. In this work, we demonstrate the diffusion-based supplementation of small molecules for the in-emulsion gelation of multiple tyramine-functionalized polymers via enzymatic crosslinking using a H_2O_2/oil nanoemulsion. This strategy is compatible with various emulsification techniques, thereby readily supporting the formation of monodisperse hydrogel particles spanning multiple length scales ranging from the nano- to the millimeter. As proof of principle, we leveraged droplet microfluidics in combination with the cytocompatible nature of enzymatic crosslinking to engineer hollow cell-laden hydrogel microcapsules that support the formation of viable and functional 3D microtissues. The straightforward, universal, and cytocompatible nature of nanoemulsion-induced enzymatic crosslinking facilitates its rapid and widespread use in numerous food, pharma, and life science applications.

Main

Introduction

Hydrogels are key to many applications in food, pharmacy, cosmetics, and tissue engineering.[1-5] These structurally stable water-swollen polymer networks have been proven ideally suited for the nano- and microencapsulation of bioactive components including cells and drugs.[6,7] The encapsulating particles are typically produced via molding, atomization, or emulsification of the hydrogel precursor solution followed by an *in situ* gelation strategy.[8-10] In particular, emulsions can be continuously produced at high rates while stabilizing surfactants make them compatible with relatively slow (seconds to minutes) gelation mechanisms such as Michael-type addition,[11] temperature-dependent gelation,[12] and enzyme-based crosslinking approaches.[13] The majority of polymer gelation strategies however requires the presence of crosslinker molecules such as ions and radicals,[14] which is not trivial in emulsions, as these are typically multiphase immiscible systems where oil hampers the direct mixing of the hydrogel precursor and its crosslinker.

The most straightforward solution to crosslink hydrogel precursor droplets in an oil phase is by adding the crosslinker immediately before emulsification.[11,15,16] However, this strategy reduces the control over the emulsification process due to increasing liquid viscosity and may result in inhomogeneous polymeric networks because the crosslinking is induced before the hydrogel precursor and its crosslinker are homogeneously mixed.[13] Furthermore, coupling gelation and emulsification frequently causes device clogging and off-center cell encapsulation, which hampers the long-term applications of cell-laden hydrogel particles.[17] Consequently, it is often desirable to sequentially perform the emulsification and gelation processes, which requires the in-emulsion generation or release of crosslinker molecules. A number of advanced strategies has been developed to enable the *in situ* presentation of a crosslinker upon a chemical or physical trigger, such as changing pH, irradiation, and temperature.[6,18-21] However, the commonly used acid-, photo-, and heat-triggered crosslinking strategies are detrimental to cell survival and function, or are

technically challenging as they require the formation of labile crosslinker-laden complexes.[13,22,23] Alternatively, gelation of emulsified hydrogel precursor droplets can be induced via the diffusion-based supplementation of crosslinker molecules, which does not depend on technically challenging or cytotoxic triggers. For example, alginate microspheres have been formed by supplementing the oil phase with crosslinker nanoparticles[24,25] and nanodroplets[26] that diffuse through the oil phase and induce crosslinking of the emulsified polymer droplets. Unfortunately, studies that reported on the in-emulsion crosslinking through diffusion of crosslinker molecules have remained limited and nearly exclusively focused on the production of alginate microparticles. Expanding the portfolio of in-emulsion diffusion-based crosslinkable materials by would facilitate numerous hydrogel-based applications.

In this work, we demonstrated the in-emulsion enzymatic crosslinking of three distinct tyramine-functionalized polymers using horseradish peroxidase (HRP) and H_2O_2 that was supplemented by diffusion from a H_2O_2/oil nanoemulsion. The crosslinker nanoemulsion was combined with various emulsification techniques to produce homogeneously crosslinked monodisperse nano-, micro-, and millimeter-sized hydrogel particles. Combining the crosslinker nanoemulsion with droplet microfluidics readily enabled the production of hollow dextran-based microcapsules that supported functional 3D microtissue formation. This confirmed the cytocompatible nature of the nanoemulsion-induced enzymatic crosslinking strategy and proved its value for 3D cell culture applications.

Results and discussion

Preparation and characterization of crosslinker nanoemulsion

Tyramine-functionalized polymers can be crosslinked *in situ* via the formation of tyramine-tyramine bonds using horseradish peroxidase (HRP) as catalyst and low levels of H_2O_2 as oxidizer (**Figure 1a**). However, this conventionally requires the mixing of these reactive components prior

to emulsification, which significantly reduces the control over the emulsification process and typically results in deformed particles or bulk gel formation that causes device clogging (Figure S1). We therefore set out to develop a facile strategy to achieve in-emulsion crosslinking of tyramine-functionalized polymers. However, this is not trivial as the oil phase prevents the direct mixing of tyramine-functionalized polymer, HRP, and H_2O_2. We hypothesized, that in-emulsion crosslinking could be achieved by combining pre-emulsified enzyme containing precursor droplets with a H_2O_2 containing oil. In concept, enzymatic crosslinking of water-in-oil precursor droplets would be induced by the diffusion-based supplementation of H_2O_2 into the enzyme containing precursor droplet, while the surfactant containing oil would prevent precursor droplet merging and ensure spherically shaped particles (**Figure 1b**). To realize this, we emulsified H_2O_2 nanodroplets in oil. Compared to microdroplets, nanodroplets are more stable and have higher surface-to-volume ratios, which ensures an adequate and constant source of H_2O_2 molecules, allowing for sustained and complete gelation of precursor droplets. We exploited sonication-based emulsification followed by centrifugation to prepare the crosslinker nanoemulsion (**Figure 1c**). Specifically, 30% H_2O_2 and hexadecane with 1% Span 80 surfactant were mixed and sonicated to produce an emulsion. Using a subsequent centrifugation step, we obtained a transparent nanoemulsion (i.e. supernatant) by separating out the microdroplets and non-emulsified aqueous phase (i.e. sediment). Analyzing the supernatant using dynamic light scattering revealed that the obtained nanoemulsion was composed of two droplet populations with diameters ranging from 1 to 10 nm and 100 to 1000 nm (**Figure 1d**). The 1 to 10 nm population, which has also been reported by others,[27] was also present in non-emulsified surfactant containing oil and likely caused by micellar formation of Span 80 surfactant. We consequently deduced that the 100 to 1000 µm fraction consisted of H_2O_2 nanodroplets or -micelles. As shown in **Figure 1e**, the presence of H_2O_2 in the nanoemulsion was confirmed using a quantitative colorimetric peroxide assay, which revealed a H_2O_2 concentration of ~1 g/l (Figure S2).

Crosslinker nanoemulsion for homogeneous enzymatic crosslinking of spherical nano-, micro-, and millimeter particles made from various tyramine-functionalized polymers

Leveraging the H_2O_2/oil nanoemulsion, we set out to demonstrate in-emulsion crosslinking of various tyramine-functionalized materials droplets for the production of monodisperse spherical particles. To extend the material compatibility of our nanoemulsion-induced crosslinking strategy, we conjugated the enzymatically crosslinkable moiety tyramine to dextran (Dex-TA), hyaluronic acid (HA-TA), and polyethylene glycol (PEG-TA), which are three distinct polymers that have been proven successful in various biomedical applications.[28-31] A facile production method based on dripping HRP containing hydrogel precursor droplets from a micropipette into a crosslinker bath was used to assess in-emulsion crosslinking of these polymer conjugates (**Figure 2a**). Dripping the polymer solutions in the H_2O_2/oil nanoemulsion resulted in the formation of shape stable spheres for all tested biomaterials (**Figure 2b-d**). Conversely, dripping in an aqueous bath (i.e. water) that had similar H_2O_2 concentration (i.e. ~ 1 g/l) resulted in amorphously shaped gel particles, confirming the important shape stabilizing role of the immiscible oil phase during crosslinking (**Figure 2e**). The structural and mechanical properties of in-emulsion crosslinked (i.e. by H_2O_2 diffusion) Dex-TA hydrogels were then compared to Dex-TA hydrogels that had been prepared using the conventional crosslinking approach (i.e. by H_2O_2 mixing) (**Figure 2f**). To evaluate the internal hydrogel structure, gel precursor droplets were cured on flat substrates and visualized using inverted phase contrast (PC) and ultraviolet (UV) fluorescence microscopy. Analyzing the relative UV intensity across the hydrogels, as a measure for dityramine (i.e. crosslinked tyramine) distribution,[32] revealed that diffusion-based crosslinking resulted a more homogeneously crosslinked hydrogel interior as compared to samples that were prepared by mixing. Moreover, nanoindentation measurements demonstrated that diffusion-based crosslinking resulted in a significantly stiffer hydrogel surface (i.e. E-modulus) as compared to the mixing strategy (**Figure 2g**). This observation was corroborated by matrix scanning indentation of the hydrogel surface, which revealed that in-emulsion crosslinking Dex-TA resulted in ~3-fold less variation in stiffness

(**Figure 2h**). These observations are likely to be explained by the fact that H_2O_2 induces relatively rapid gelation that prevents thorough mixing of all reactive components, thereby resulting in an inhomogeneous polymer network when applying the conventional mixing approach, whereas nanoemulsion-based crosslinking relies on the diffusion-based gelation of a premixed gel precursor solution.

As the precursor droplets and crosslinker nanoemulsion are produced separately, the nanoemulsion-induced crosslinking is readily compatible with a wide variety of emulsion-based droplet production technologies. Indeed, spherical particles ranging from the nano- to the millimeter scale could be produced by combining various existing emulsion-based droplet production technologies using a chemically identical crosslinker nanoemulsion. In particular, we used sonication (**Figure 3a, b**), droplet microfluidics (**Figure 3c-e**), and dripping (**Figure 3f, g**) in combination with nanoemulsion based enzymatic crosslinking to demonstrate the production of monodisperse spherical Dex-TA particles with diameters spanning at least four orders of magnitude (**Figure 3h**). The generic nature of this crosslinking strategy facilitates its application in various fields that rely on the use of emulsion-based particle production including pharma, tissue engineering, and food technology.[33-37]

Producing hollow hydrogel microcapsules using nanoemulsion-induced enzymatic crosslinking

Nanoemulsion-induced enzymatic crosslinking is intrinsically an outside-in process; H_2O_2 diffuses from the oil phase into the gel precursor droplet where it drives the HRP-mediated crosslinking of tyramines (**Figure 4a**). Inhibiting this crosslinking mechanism from the inside (i.e. the aqueous phase) using the H_2O_2 neutralizing enzyme catalase is a proven strategy to form hollow particles or capsules (**Figure 4b**).[38,39] We set out to exploit this approach in combination with droplet microfluidics to realize the production of hollow Dex-TA microcapsules. To this end, we designed and manufactured a dedicated microfluidic chip from polydimethylsiloxane (PDMS) and glass (**Figure 4c**). The microfluidics chip contained several filters to prevent any particles larger than ~50

μm in the oil phase (e.g. remaining PDMS particles from inlet punching) from interfering with the droplet generation or crosslinking processes (**Figure 4d**). Furthermore, the aqueous phase inlet contained a previously reported pillar structure [13] that ensured particle homogenization to aid evenly distributed encapsulation of particles (e.g. cells) (**Figure 4e**). The flow focusing droplet generator (**Figure 4f**) was positioned a few millimeters upstream of the crosslinker nanoemulsion inlet (**Figure 4g**). This separation between droplet production and crosslinking initiation effectively prevented flow instabilities and clogging by preventing polymer gelation at the nozzle. First, we assessed the production of non-laden (i.e. without cells) hydrogel microcapsules. After Dex-TA, HRP, and catalase containing gel precursor droplets were stabilized, on-chip enzymatic crosslinking was induced by introducing H_2O_2/oil nanoemulsion (~1 g/l) in the serpentine-shaped delay channel with an nanoemulsion/oil flow ratio of 1:8 (**Figure 4h**). The nanoemulsion's slightly diffuse appearance was no longer observed after four channel turns (i.e. 20 mm), which indicated its homogenous distribution across the microfluidic delay channel. The resulting 75±1 μm spherical particles were retrieved by washing the collected emulsion with surfactant-free oil and breaking it in the presence of phosphate-buffered saline (PBS) (**Figure 4i**). Analyzing these particles using confocal microscopy revealed the presence of homogeneously crosslinked shells of even thickness (8±1 μm) surrounding a non-crosslinked core, confirming the controlled production of hollow Dex-TA microcapsules (**Figure 4j**).

Engineering functional 3D microtissues in hollow hydrogel microcapsules via nanoemulsion-induced crosslinking

Hollow microcapsules are ideally suited for the controlled formation of 3D microtissues,[25,26,40] which serve multiple purposes in fundamental biological, pharmacological, and tissue engineering applications.[41-43] For example, controlled aggregation of cells is key to bottom-up engineering of islets of Langerhans for the treatment of diabetes.[44,45] To investigate the potential of nanoemulsion-induced enzymatic crosslinking for 3D cell cultures, we set out to encapsulate the

pancreatic beta cell line MIN6 to form insulin producing microtissues. First, we aimed to identify the smallest amount of H_2O_2 containing nanoemulsion that still resulted in robust cell encapsulating microcapsules, as even a small excess of H_2O_2 (order 1 to 10 mg/l) has been proven detrimental to cell functioning.[46] The separated configuration of droplet generator and nanoemulsion inlet enabled straightforward screening of increasing amounts of crosslinker without affecting droplet size. Specifically, cell-laden gel precursor droplets were produced using a constant water/oil ratio of 1:8, while the nanoemulsion/oil ratio was stepwise increased from 1:16 to 1:2 (**Figure 5a**). Collecting the on-chip formed samples in an off-chip aqueous bath (i.e. cell culture medium) resulted in <25% encapsulated cells in all tested nanoemulsion/oil ratios (**Figure 5b**). This poor cell encapsulation was most likely the result of incomplete on-chip crosslinking and immediate demulsification upon collection in the serum-containing aqueous bath. However, by collecting the emulsion in an oil bath, immediate demulsification could be prevented. This approach effectively increased the enzymatic crosslinking time of cell-laden droplets from seconds (on-chip) to minutes (in-suspension) resulting in robust Dex-TA microcapsules that encapsulated ~90% of the cells while using minimal amounts of H_2O_2. Using this optimized encapsulation strategy, we compared viability rates of encapsulated to non-encapsulated (i.e. syringe control) cells using a live/dead assay (**Figure 5c**). This revealed that the encapsulation procedure had no detrimental effect on cell survival (**Figure 5d**). The encapsulated cells autonomously assembled into 3D microtissues within a single day (**Figure 5e**) and continued to proliferate during subsequent *in vitro* culture (**Figure 5f**), which significantly increased the cell aggregates' size (**Figure 5g**). KI67 staining revealed that MIN6 cells intensively proliferated as early as day 1 post encapsulation, which underlined the cytocompatible nature of the nanoemulsion-induced enzymatic crosslinking strategy (**Figure 5h**). Importantly, encapsulated and aggregated MIN6 cells remained positive for insulin staining throughout the culture period, indicating that the MIN6 cells remained functional during encapsulation and subsequent culture, further confirming the mild and cytocompatible nature of the procedure (**Figure 5i**).

Conclusion

In conclusion, we demonstrated the successful preparation and application of nanoemulsified H_2O_2 for the in-emulsion enzymatic crosslinking of tyramine-functionalized polymers including dextran (Dex-TA), hyaluronic acid (HA-TA), and polyethylene glycol (PEG-TA). In-emulsion enzymatic crosslinking readily enabled monodisperse spherical particle formation over a size range spanning at least 4 orders (nm to mm). Furthermore, diffusion-based crosslinking resulted in more homogenously crosslinked Dex-TA hydrogels that yielded higher and more consistent Young's moduli as compared to the conventional hydrogel preparation method. Lastly, we introduced the crosslinker nanoemulsion in a microfluidic chip and leveraged its cytocompatible nature to produce cell-laden hollow microcapsules that facilitated the controlled formation of viable and functional 3D microtissues. In short, we demonstrated that a H_2O_2/oil nanoemulsion enabled facile, homogeneous, and cytocompatible in-emulsion enzymatic crosslinking of multiple distinct hydrogel precursor polymer droplets to form solid and hollow spherical particles with diameters ranging from the nano- to the millimeter scale.

Experimental section

Materials: Dex-TA, HA-TA, and PEG-TA were synthesized as previously described.[47-49] The resulting Dex-TA and HA-TA contained 15 and 3 tyramine moieties per 100 repetitive units, respectively. PEG-TA contained 5 tyramine moieties per 8-armed PEG molecule. Horseradish peroxidase (HRP, type VI), H_2O_2 (with inhibitor), hexadecane, Span 80, peroxide color indicator strips (Quantofix), fetal bovine serum (FBS), iodixanol (OptiPrep), Calcein-AM, ethidium homodimer-1 (EthD-1), buffered formalin, Triton X-100, Tween 20, and bovine serum albumin (BSA) were purchased from Sigma-Aldrich. Catalase (from bovine liver) was purchased from Wako. Phosphate-buffered saline (PBS) was purchased from Lonza. Dulbecco's Modified Eagle's Medium (DMEM), Minimal Essential

Medium α with nucleosides (αMEM), Penicillin and Streptomycin, GlutaMAX, 2-mercaptoethanol, HEPES, and trypsin-EDTA were purchased from Gibco. Basic fibroblast growth factor (ISOKine bFGF) was purchased from Neuromics. Anti-KI67-FITC (556026) was purchased from BD Biosciences. Anti-insulin (AB7842) was purchased from Abcam. Fluorescently labeled phalloidin and secondary antibodies were purchased from purchased from Molecular Probes. DAPI was purchased from Invitrogen. Polydimethylsiloxane (PDMS, Sylgard 184) was purchased from Dow Corning. Aquapel was purchased from Vulcavite.

Preparation and characterization of crosslinker nanoemulsion: Crosslinker emulsion was prepared by mixing 30% (w/v) H_2O_2 and 1% (v/v) Span 80 containing hexadecane in a 1:5 volume ratio using a p1000 micropipette, and subsequent sonication for 5 minutes (Engisonic 200, 30 W, 47 kHz), mixing by shaking, and again 5 minutes sonication. To obtain a pure nanoemulsion, microdroplets were removed by 5 minutes centrifugation at 2000g. The size distribution of the obtained nanoemulsion was analyzed by measuring a 100 times diluted sample using dynamic light scattering (Zetasizer Nano ZS, Malvern). As a blank control, we measured surfactant containing hexadecane that was not emulsified with H_2O_2. The H_2O_2 concentration of the nanoemulsion was quantified using a color indicator strip that was pre-wetted with demineralized water.

Preparation and characterization of solid hydrogel particles: Millimeter-sized particles were produced by dripping 10 µl hydrogel precursor polymer droplets that consisted of 10% (w/v) tyramine-functionalized polymer and 11 U/ml HRP in PBS into H_2O_2/oil nanoemulsion. Alternatively, millimeter-sized particles were produced by putting 10 µl hydrogel precursor droplets that contained premixed 10% (w/v) Dex-TA and 11 U/ml HRP on a polystyrene substrate and subsequently covering them with 1 g/l H_2O_2 nanoemulsion. Millimeter-sized particles were also produced by mixing 10% (w/v) Dex-TA, 11 U/ml HRP, and 0.06% (w/v) H_2O_2 in 10 µl droplets using at least 10 times vigorous pipetting on a polystyrene substrate on ice, followed by a post-cure with 0.06% (w/v) H_2O_2 in PBS. Nanoparticles were produced by mixing H_2O_2/oil nanoemulsion with hydrogel precursor

nanoemulsion that were prepared using the same sonication and centrifugation protocol. Microparticles were produced using a microfluidic droplet generator, where hydrogel precursor solution and H_2O_2/oil nanoemulsion were used as the dispersed and continuous phase at a 1:8 flow ratio, respectively. Alternatively, the continuous phase was 1% (v/v) Span 80 containing hexadecane and crosslinking was induced by introduction of H_2O_2/oil nanoemulsion using a separate inlet in the delay channel downstream of the droplet generator. Solidified hydrogel particles were separated from the oil phase by washing with surfactant-free oil in the presence of PBS. To retrieve the nanoparticles, a small amount of 2-propanol was added to the PBS. Crosslinked tyramines (i.e. dityramines) autofluoresce under ultraviolet (UV) light with excitation maximum at 315 nm and emission maximum at 405 nm.[32] To analyze the internal structure of millimeter-sized hydrogels, 10 µl hydrogel precursor droplets on flat polystyrene substrates were crosslinked and visualized using inverted phase contrast (PC) and fluorescence microscopy (EVOS FL with DAPI light cube). The relative UV intensity (i.e. intensity / average intensity) across hydrogels was measured using ImageJ. For nanoindentation, millimeter-sized hydrogels were placed on a glass stage in PBS and measured on at least four locations using a probe with a cantilever stiffness of 18.7 N/m and a diameter of 214 µm (Piuma, Optics11). Effective Young's moduli were determined by applying the Oliver-Pharr theory on the unloading part of indentation curves that were obtained using the following piezo indentation sweep settings (relative to piezo position set point at start): D[Z1] = 0 nm, t[1] = 2.0 s; D[Z2] = 15,000 nm, t[2] = 1.0 s (loading); D[Z3]= 15,000 nm, t[3] = 7.0 s (holding); D[Z4] = 0 nm, t[4] = 20.0 s (unloading); D[Z5] =0 nm, t[5] 2.0 s. To determine the variation in stiffness (coefficient of variation), matrix indentation was performed on at least 16 positions spaced 300 µm apart using the same indentation protocol and a probe with a cantilever stiffness of 24.5 N/m and a diameter of 70 µm. Size distributions of nano- and micro-, and millimeter-sized particles were determined using dynamic light scattering and phase contrast microscopy in combination with a Matlab function for circle size analysis (imfindcircles.m), respectively.

Preparation of microfluidic chips: Microfluidic chip designs were made using CAD software (Clewin, WieWeb) and chips with 100 µm high channels were manufactured from PDMS and glass using standard soft lithography techniques. Aquapel was introduced in the chips before usage to ensure channel wall hydrophobicity. Chips were connected to gastight syringes (Hamilton) using fluorinated ethylene propylene (FEP, inner diameter 250 µm, DuPont), which were controlled by low pressure syringe pumps (neMESYS, Cetoni).

Preparation of (cell-laden) microcapsules: Hydrogel precursor solution that consisted of 5% (w/v) Dex-TA, 22 U/ml HRP, and 83,000 U/ml catalase in PBS was emulsified with 1% (v/v) containing hexadecane using a microfluidic droplet generator at a 1:6 precursor/oil flow ratio. The non-cell-laden precursor droplets were crosslinked by the influx of crosslinker nanoemulsion at a 1:8 nanoemulsion/oil flow ratio further downstream the delay channel, resulting in Dex-TA microcapsules through competitive enzymatic crosslinking. For cell-laden microcapsule production, mouse insulinoma MIN6-B1 cells were cultured in MIN6 proliferation medium, consisting of 10% (v/v) FBS, 100 U/ml Penicillin and 100 mg/ml Streptomycin, and 71 µM 2-mercaptoethanol (added fresh) in DMEM. Cells were cultured under 5% CO_2 at 37 °C and medium was replaced 3 times per week. When cell culture reached near confluence, the cells were detached using 0.25% Trypsin-EDTA at 37 °C and subsequently subcultured or used for experimentation. For cell encapsulation, detached cells (passage 35) were washed with MIN6 proliferation medium, flown through a 40 µm cell strainer, and suspended in the hydrogel precursor solution (to which 8% (v/v) OptiPrep was added to obtain ρ = 1.05 g/l which reduces cell settling and aggregation) at a concentration of $7.5 \cdot 10^7$ cells/ml. The cell-laden hydrogel precursor solution was loaded into an ice-cooled gastight syringe where it was gently agitated every ten minutes using a magnetic micro stirring bar. The cell-laden precursor droplets were crosslinked by the influx of crosslinker nanoemulsion at various nanoemulsion/oil flow ratios as indicated in Figure 5. The resulting microcapsules were collected in MIN6 proliferation medium supplemented with 0.02 M HEPES or in surfactant containing hexadecane. To break the emulsion and retrieve the microcapsules from

the oil phase, microcapsules were washed with surfactant-free oil in the presence of PBS or MIN6 proliferation medium. Retrieved cell-laden microcapsules were cultured in MIN6 proliferation medium which was refreshed three times per week.

Staining and visualization: Millimeter-sized particles were imaged using a standard digital photo camera. On-chip droplets and microgels were visualized using a stereomicroscope set-up (Nikon SMZ800 equipped with Leica DFC300 FX camera). Nanoparticles were washed with water, air-dried and subsequently imaged using scanning electron microscopy (Zeiss Merlin HR-SEM) at 0.65 kV. Collected microemulsions and -particles were imaged using phase contrast microscopy. Microcapsules were analyzed by selectively labeling crosslinked Dex-TA with EthD-1 and visualization using confocal microscopy (Nikon A1+). Optical cross sections were analyzed using ImageJ. Viability of encapsulated cells was analyzed by staining with 2 µM calcein-AM and 4 µM EthD-1 in PBS, visualization using fluorescence microscopy (EVOS FL), and artisan counting of > 300 cells per condition. For additional analyses, cell-laden microgels were first washed with PBS and fixated using 10% buffered formalin. For immunohistochemistry, samples were permeabilized with 0.1% Triton X-100, blocked with 5% (w/v) bovine serum albumin and 0.05% (v/v) Tween 20, and stained with 1:100 anti-KI67-FITC (556026, BD Biosciences), 1:100 anti-insulin (AB7842, Abcam), in combination with 1:400 AF647-labeled secondary antibodies, and 2.5 U/ml phalloidin-AF488 and DAPI to counterstain F-actin, and nuclei, respectively. MIN6 aggregate size distributions were determined by measuring the surface area of >50 aggregates per condition using ImageJ, represented as box plots, and analyzed for statistical significance using one-way ANOVA.

Acknowledgements

We acknowledge Dr. P. Halban (Dept. of Genetic Medicine and Development, University of Geneva, Geneva, Switzerland) for providing mouse MIN6-B1 cells. We thank M.A. Smithers for his expertise in scanning electron microscopy (MESA+ Institute for Nanotechnology, University of

Twente). We gratefully acknowledge the funding from the Dutch Diabetes Research Foundation, as part of the Diabetes Cell Therapy Initiative, and the Dutch Arthritis Foundation (#12-2-411 to JL and MK and #LLP-25 to MK). JL acknowledges financial support from Innovative Research Incentives Scheme Veni (#14328) from the Netherlands Organization for Scientific Research (NWO).

Author contributions

Conception by TK, SH, and JL. Experiments by TK, SH, BZ, NR, RW, and BP. Data interpretation by all authors. First draft by TK, SH, and JL. Supervision and revisions by HW, MK, and JL.

Competing financial interests

The authors declare no competing financial interests.

Supporting Information

Supporting Information is available from the publisher or from the author.

References

1. A. S. Hoffman, *Advanced drug delivery reviews*, 2012, **64**, 18-23.
2. L. S. Liu, J. Kost, F. Yan and R. C. Spiro, *Polymers-Basel*, 2012, **4**, 997-1011.
3. L. Yu and J. D. Ding, *Chemical Society reviews*, 2008, **37**, 1473-1481.
4. N. A. Peppas, J. Z. Hilt, A. Khademhosseini and R. Langer, *Adv Mater*, 2006, **18**, 1345-1360.
5. S. R. Van Tomme, G. Storm and W. E. Hennink, *Int J Pharm*, 2008, **355**, 1-18.
6. W. H. Tan and S. Takeuchi, *Adv Mater*, 2007, **19**, 2696-+.
7. M. Hamidi, A. Azadi and P. Rafiei, *Advanced drug delivery reviews*, 2008, **60**, 1638-1649.
8. S. Selimovic, J. Oh, H. Bae, M. Dokmeci and A. Khademhosseini, *Polymers-Basel*, 2012, **4**, 1554-1579.
9. A. C. Lima, P. Sher and J. F. Mano, *Expert opinion on drug delivery*, 2012, **9**, 231-248.
10. J. K. Oh, R. Drumright, D. J. Siegwart and K. Matyjaszewski, *Prog Polym Sci*, 2008, **33**, 448-477.

11. T. Rossow, J. A. Heyman, A. J. Ehrlicher, A. Langhoff, D. A. Weitz, R. Haag and S. Seiffert, *J Am Chem Soc*, 2012, **134**, 4983-4989.
12. A. Kumachev, J. Greener, E. Tumarkin, E. Eiser, P. W. Zandstra and E. Kumacheva, *Biomaterials*, 2011, **32**, 1477-1483.
13. S. Henke, J. Leijten, E. Kemna, M. Neubauer, A. Fery, A. van den Berg, A. van Apeldoorn and M. Karperien, *Macromolecular bioscience*, 2016, DOI: 10.1002/mabi.201600174.
14. W. E. Hennink and C. F. van Nostrum, *Advanced drug delivery reviews*, 2012, **64**, 223-236.
15. Y. Ma, M. P. Neubauer, J. Thiele, A. Fery and W. T. S. Huck, *Biomaterials Science*, 2014, **2**, 1661-1671.
16. D. R. Griffin, W. M. Weaver, P. O. Scumpia, D. Di Carlo and T. Segura, *Nature materials*, 2015, **14**, 737-+.
17. T. Kamperman, S. Henke, C. W. Visser, M. Karperien and J. Leijten, *Small*, 2017, DOI: 10.1002/smll.201603711, 1603711-n/a.
18. A. Johansen and J. M. Flink, *Enzyme Microb Tech*, 1986, **8**, 145-148.
19. S. Utech, R. Prodanovic, A. S. Mao, R. Ostafe, D. J. Mooney and D. A. Weitz, *Advanced healthcare materials*, 2015, **4**, 1628-1633.
20. T. Kamperman, S. Henke, A. van den Berg, S. R. Shin, A. Tamayol, A. Khademhosseini, M. Karperien and J. Leijten, *Advanced healthcare materials*, 2017, **6**.
21. S. Ma, M. Natoli, X. Liu, M. P. Neubauer, F. M. Watt, A. Fery and W. T. S. Huck, *Journal of Materials Chemistry B*, 2013, **1**, 5128-5136.
22. T. Gu, E. W. Yeap, A. Somasundar, R. Chen, T. A. Hatton and S. A. Khan, *Lab Chip*, 2016, **16**, 2694-2700.
23. C. D. Ren, M. Kurisawa, J. E. Chung and J. Y. Ying, *Journal of Materials Chemistry B*, 2015, **3**, 4663-4670.
24. J. P. Paques, E. van der Linden, C. J. M. van Rijn and L. M. C. Sagis, *Food Hydrocolloid*, 2013, **31**, 428-434.
25. P. Agarwal, S. T. Zhao, P. Bielecki, W. Rao, J. K. Choi, Y. Zhao, J. H. Yu, W. J. Zhang and X. M. He, *Lab Chip*, 2013, **13**, 4525-4533.
26. S. Sakai, I. Hashimoto, Y. Ogushi and K. Kawakami, *Biomacromolecules*, 2007, **8**, 2622-2626.
27. B. R. Solomon, N. Hyder and K. K. Varanasi, *Scientific reports*, 2014, **4**.
28. C. C. Lin and K. S. Anseth, *Pharm Res-Dord*, 2009, **26**, 631-643.
29. J. A. Cadee, M. J. A. van Luyn, L. A. Brouwer, J. A. Plantinga, P. B. van Wachem, C. J. de Groot, W. den Otter and W. E. Hennink, *J Biomed Mater Res*, 2000, **50**, 397-404.
30. K. J. Portalska, L. M. Teixeira, J. C. Leijten, R. Jin, C. van Blitterswijk, J. de Boer and M. Karperien, *Tissue engineering. Part A*, 2014, **20**, 819-829.
31. J. A. Burdick and G. D. Prestwich, *Adv Mater*, 2011, **23**, H41-H56.
32. D. V. Sakharov, A. Bunschoten, H. van Weelden and K. W. A. Wirtz, *Eur J Biochem*, 2003, **270**, 4859-4865.
33. H. M. Shewan and J. R. Stokes, *J Food Eng*, 2013, **119**, 781-792.
34. S. M. Joscelyne and G. Tragardh, *J Membrane Sci*, 2000, **169**, 107-117.
35. S. Freitas, H. P. Merkle and B. Gander, *Journal of Controlled Release*, 2005, **102**, 313-332.
36. S. Y. Teh, R. Lin, L. H. Hung and A. P. Lee, *Lab Chip*, 2008, **8**, 198-220.
37. A. Khademhosseini and R. Langer, *Biomaterials*, 2007, **28**, 5087-5092.
38. T. Ashida, S. Sakai and M. Taya, *Biotechnol Prog*, 2013, **29**, 1528-1534.
39. M. Khanmohammadi, S. Sakai, T. Ashida and M. Taya, *J Appl Polym Sci*, 2016, **133**.
40. S. Sakai, S. Ito, H. Inagaki, K. Hirose, T. Matsuyama, M. Taya and K. Kawakami, *Biomicrofluidics*, 2011, **5**, 13402.
41. P. Occhetta, M. Centola, B. Tonnarelli, A. Redaelli, I. Martin and M. Rasponi, *Scientific reports*, 2015, **5**, 10288.
42. Y. C. Tung, A. Y. Hsiao, S. G. Allen, Y. S. Torisawa, M. Ho and S. Takayama, *The Analyst*, 2011, **136**, 473-478.

43. F. Wolf, C. Candrian, D. Wendt, J. Farhadi, M. Heberer, I. Martin and A. Barbero, *European cells & materials*, 2008, **16**, 92-99.
44. T. Toyoda, S. Mae, H. Tanaka, Y. Kondo, M. Funato, Y. Hosokawa, T. Sudo, Y. Kawaguchi and K. Osafune, *Stem cell research*, 2015, **14**, 185-197.
45. J. Hilderink, S. Spijker, F. Carlotti, L. Lange, M. Engelse, C. van Blitterswijk, E. de Koning, M. Karperien and A. van Apeldoorn, *Journal of cellular and molecular medicine*, 2015, **19**, 1836-1846.
46. J. Duan, Z. Zhang and T. Tong, *The international journal of biochemistry & cell biology*, 2005, **37**, 1407-1420.
47. R. Wang, DOI: 10.3990/1.9789036540230, University of Twente, 2016.
48. R. Jin, C. Hiemstra, Z. Y. Zhong and J. Feijen, *Biomaterials*, 2007, **28**, 2791-2800.
49. J. W. H. Wennink, K. Niederer, A. I. Bochynska, L. S. M. Teixeira, M. Karperien, J. Feijen and P. J. Dijkstra, *Macromol Symp*, 2011, **309-310**, 213-221.

Figures

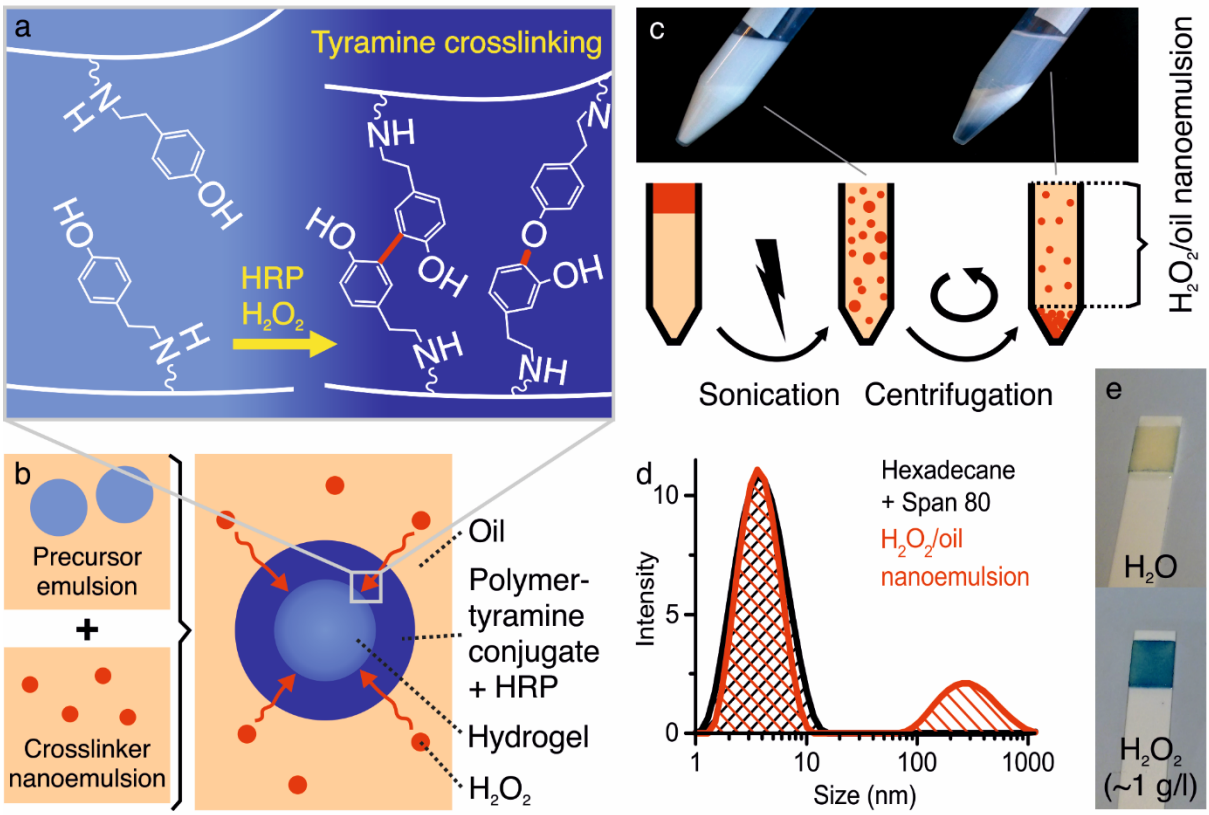

Figure 1. Preparation, and characterization of crosslinker nanoemulsion. (**a**) Tyramine moieties are crosslinked by the enzyme HRP in the presence of H_2O_2. (**b**) Concept of in-emulsion crosslinking HRP containing hydrogel precursor droplets using a H_2O_2/oil nanoemulsion (**c**). The nanoemulsion is prepared and purified by sonication-mediated emulsification of H_2O_2 in oil and subsequent centrifugation. (**d, e**) The presence of 1 g/l H_2O_2 containing nanoemulsion was confirmed using dynamic light scattering and a quantitative colorimetric peroxide assay.

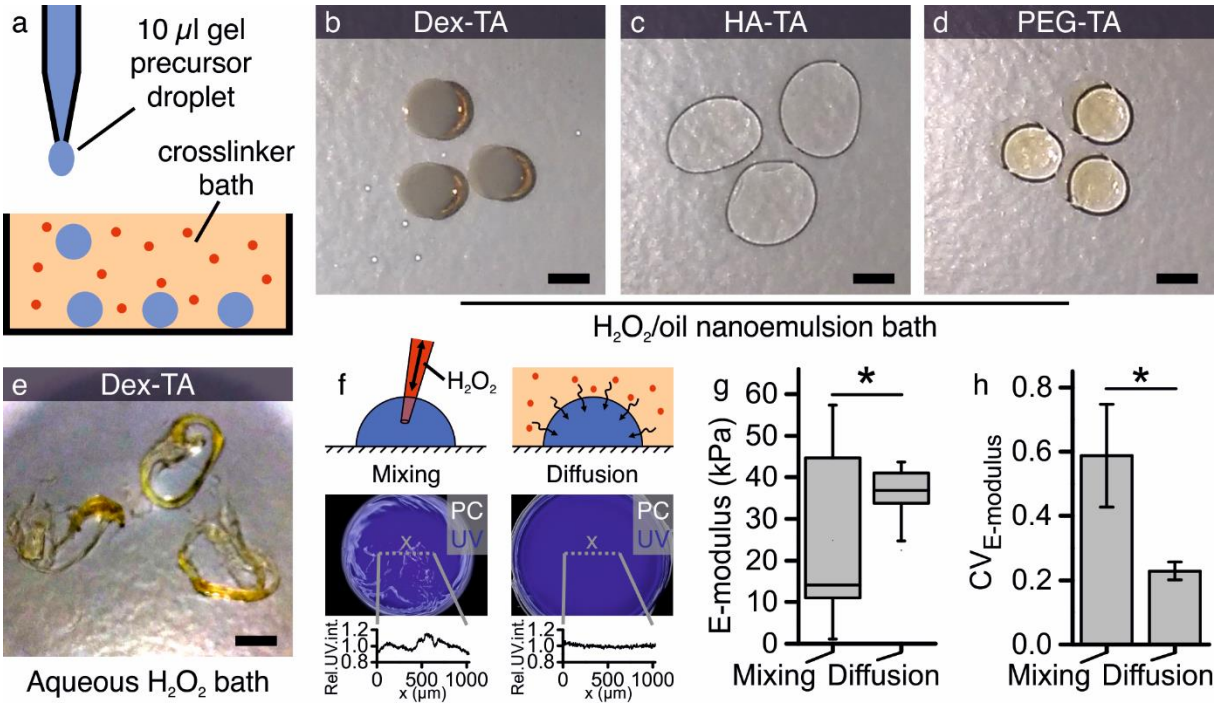

Figure 2. Spherical and homogeneous particle production using nanoemulsion-induced enzymatic crosslinking. (**a**) Dripping HRP containing tyramine-functionalized hydrogel precursor solutions from a micropipette into a H_2O_2/oil nanoemulsion bath resulted in spherical (**b**) Dex-TA, (**c**) HA-TA, and (**d**) PEG-TA particles, (**e**) which was in sharp contrast to the amorphously shaped particles that formed upon dripping the same Dex-TA precursor solution into an aqueous bath with similar H_2O_2 concentration as the H_2O_2/oil nanoemulsion bath. (**f**) The conventional hydrogel preparation method (i.e. mixing) was compared to diffusion-based crosslinking. To study the intrinsic hydrogel crosslinking (i.e. dityramine) distribution, hydrogels were prepared on top of flat substrates and analyzed in a cross manner sectional using inverted phase contrast (PC) and ultraviolet (UV) fluorescence microscopy. Nanoemulsion-induced crosslinking resulted in a more homogeneously crosslinked hydrogel interior as compared to mixing. Furthermore, (**g**) hydrogels prepared using diffusion-based crosslinking were significantly stiffer and (**h**) characterized by significantly less spreading (coefficient of variation; CV) than hydrogels prepared by directly mixing the gel precursor with a non-emulsified H_2O_2 solution. * indicates significance between populations with $p<0.05$. Black scale bars indicate 2 mm.

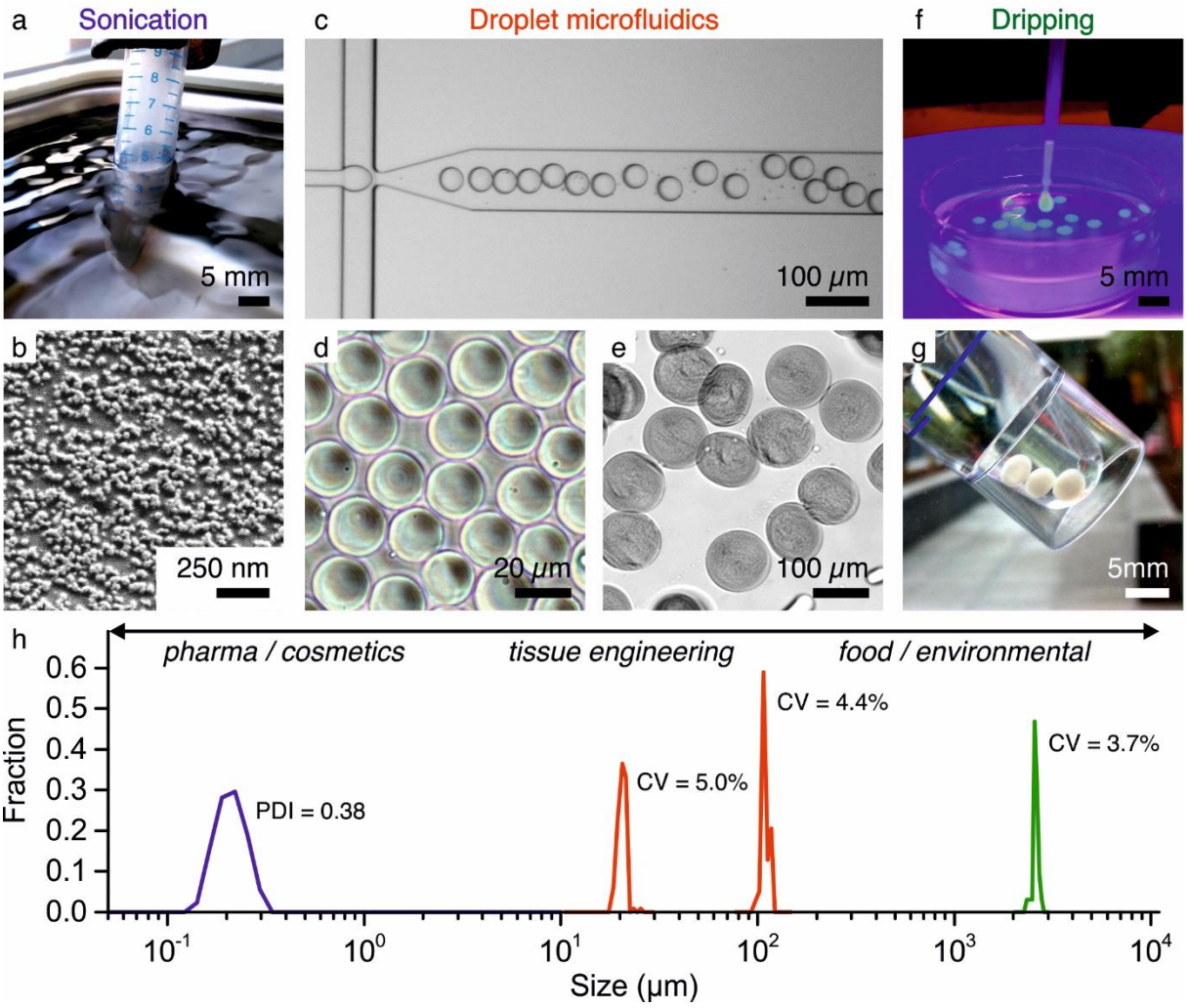

Figure 3. Monodisperse nano-, micro-, and millimeter particle production using nanoemulsion-induced enzymatic crosslinking. (**a**) Mixing HRP and Dex-TA containing nanoemulsion prepared using sonication resulted in (**b**) Dex-TA nanoparticles when mixed with H_2O_2/oil nanoemulsion, as confirmed with scanning electron microscopy. (**c**) Droplet microfluidics was used to generate (**d**) 20 μm and (**e**) 100 μm Dex-TA microparticles using H_2O_2/oil nanoemulsion as the continuous phase. (**f**) Dripping hydrogel precursor solution into a H_2O_2/oil nanoemulsion bath resulted in (**g**) spherical millimeter-sized particles. (**h**) Size distributions of Dex-TA particles produced with various emulsification-based technologies in combination with in-emulsion enzymatic crosslinking using crosslinker nanoemulsion. PDI indicates polydispersity index. CV indicates coefficient of variation.

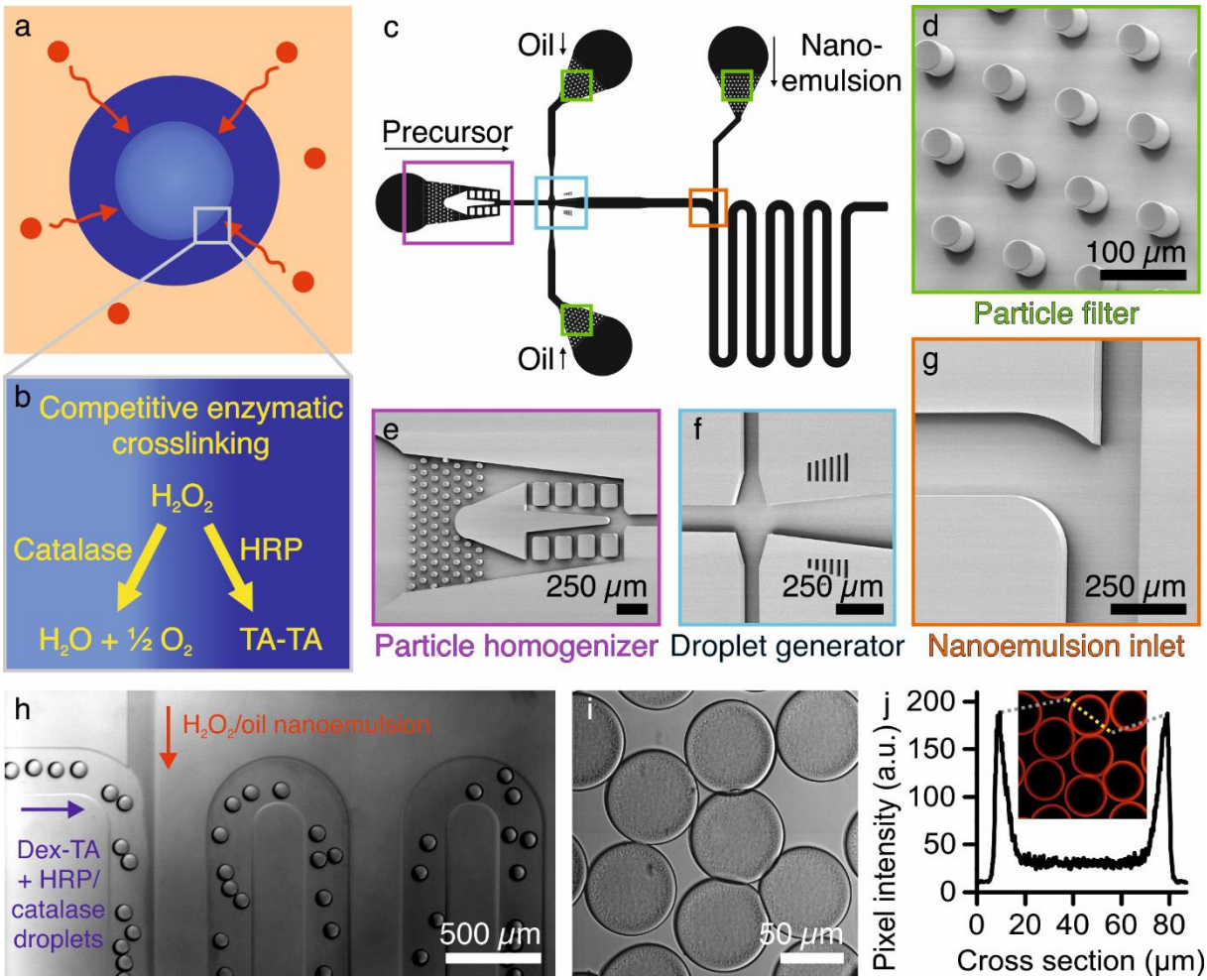

Figure 4. Hollow microcapsules production using nanoemulsion-induced enzymatic crosslinking. (**a**) Nanoemulsion-induced crosslinking is an outside-in process where small H_2O_2 molecules diffuse from the nanoemulsion through the oil phase into the gel precursor droplet to induce enzymatic crosslinking. (**b**) The enzyme catalase consumes H_2O_2 and can be incorporated in the gel precursor to achieve competitive enzymatic crosslinking that results in hollow hydrogel capsule formation. (**c**) The microfluidic microcapsule production chip containing (**d**) oil inlets with particle filters, (**e**) a gel precursor inlet with particle homogenizer, (**f**) a flow focusing droplet generator, and (**g**) an inlet for the crosslinker nanoemulsion, as shown by a schematic depiction and scanning electron microscopy images, respectively. **(h)** Microphotograph of the microfluidic chip in action, where Dex-TA, HRP, and catalase containing precursor droplets in oil (blue arrow) are solidified after the influx of H_2O_2/oil nanoemulsion (red arrow) into (**i**) robust microcapsules with (**j**) non-crosslinked centers, as confirmed by confocal imaging of the retrieved hydrogels.

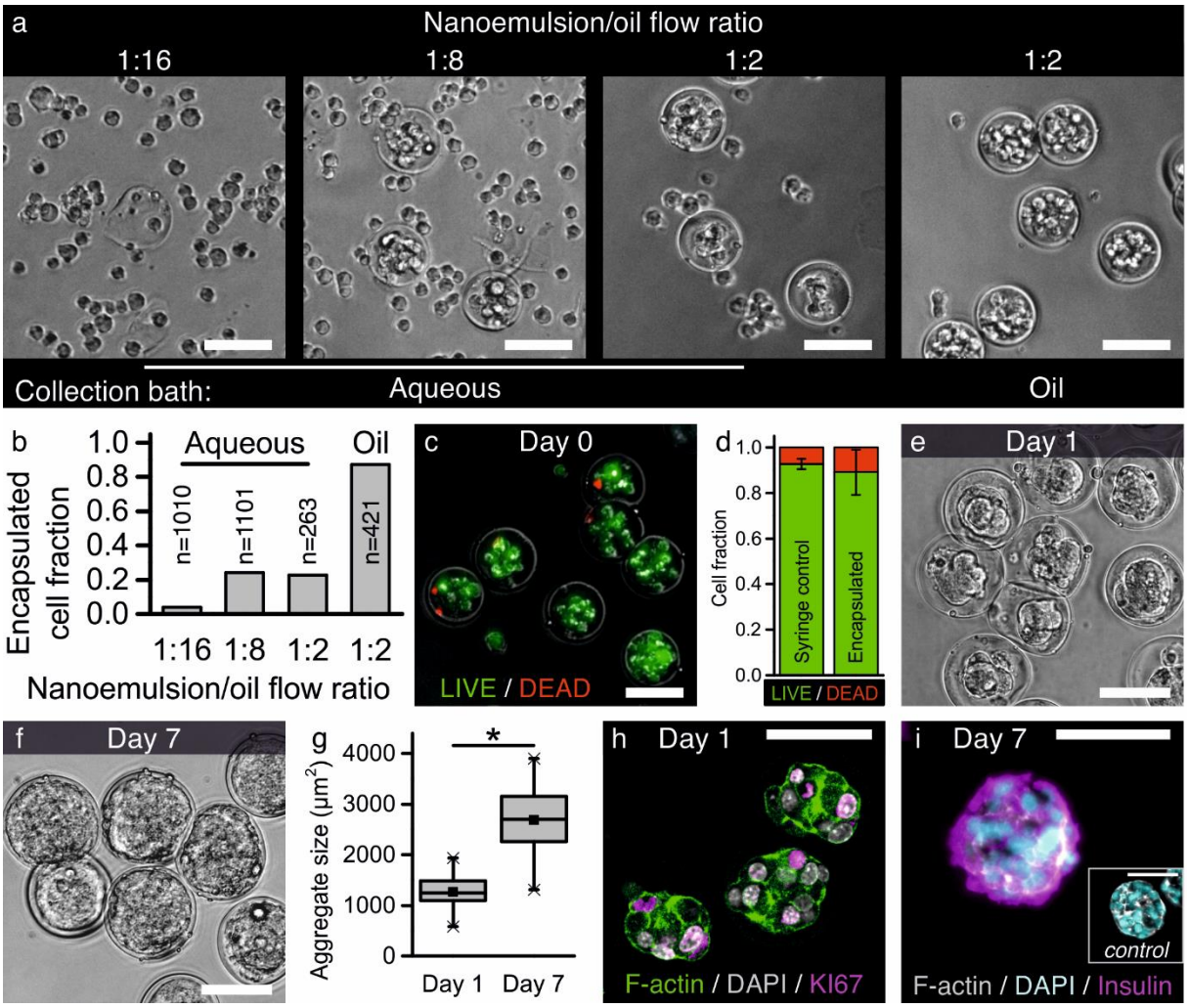

Figure 5. Functional 3D microtissue formation in hollow microcapsules. (**a**) Hollow microcapsule formation was optimized by tuning the nanoemulsion/oil flow ratio and changing the off-chip collection bath from aqueous culture medium to surfactant containing oil, (**b**) while quantifying the fraction of encapsulated cells in collected samples. (**c**) The viability of microencapsulated MIN6 cells was (**c**) visualized and (**d**) quantified using live/dead staining and compared to non-encapsulated cells (i.e. syringe control). (**e**) Within one day, encapsulated MIN6 cells formed microaggregates that (**f, g**) significantly grew during subsequent *in vitro* culture as a result of (h) cell proliferation, which was confirmed by (**h**) KI67-positive cells in the 3D microtissues on day 1. (**i**) The MIN6 cells remained viable and functional throughout the encapsulation procedure and subsequent culture, as confirmed by insulin-positive 3D microtissues on day 7. Scale bars indicate 50 μm. * indicates significance with $p<0.001$.

Supporting Information

Nanoemulsion-induced Enzymatic Crosslinking of Tyramine-functionalized Polymer Droplets

Tom Kamperman[†]*, Sieger Henke*[†]*, Bram Zoetebier, Niels Ruiterkamp, Rong Wang, Behdad Pouran, Harrie Weinans, Marcel Karperien***, and Jeroen Leijten**

[†] TK and SH contributed equally to this work

* JL and MK are shared senior author

Content: Figure S1, S2

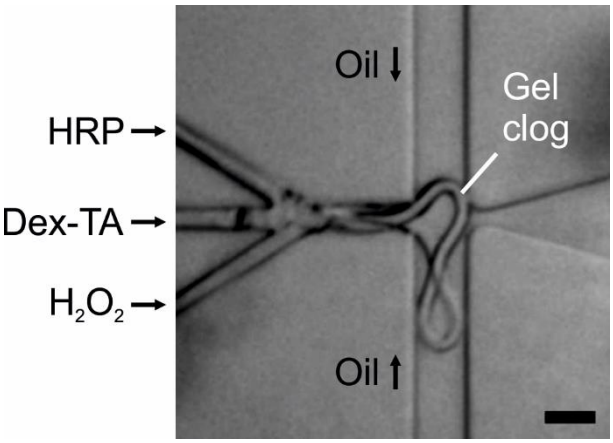

Figure S1. Mixing HRP, Dex-TA, and H_2O_2 typically results in clogging of the microfluidic droplet generator, thereby hampering its further use for hydrogel microparticle production.

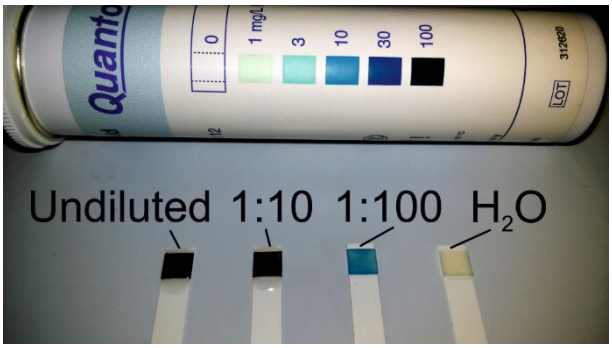

Figure S2. H_2O_2/oil nanoemulsion contained ~1 g/l H_2O_2, as determined using a 100x diluted emulsion on a quantitative peroxide color indicator strip.